ID 1654

Compressive Behavior of Composite Laminates with Different size multiple delaminations

Hiroshi Suemasu, Yoichi Osada and Hidetoshi Wakabayashi
Department of Mechanical Engineering, Faculty of Science and Technology, Sophia University
7-1 Kioicho Chiyodaku Tokyo 102, Japan

Keyword : Composite laminate, Buckling, Postbuckling, Multiple delaminations, CAI.

ABSTRACT

Postbuckling behavior of rectangular composite plates with multiple circular delaminations is studied experimentally and numerically by using finite element method. Embedded circular delaminations are placed at regular intervals in the thickness direction at the plate center. The diameter of the delamination increases from the top surface to the other surface as usually observed in the impact damage in composite laminates. The effect of size difference of the delaminations on the compressive behavior is investigated. A three-dimensional block element is adopted in the finite element analysis in order to accurately obtain distributions of each component of energy release rate along the delamination fronts. The contact problem of the delaminated surface is approximately considered by placing spring elements between the nodes at the upper and lower surfaces of delaminations, which has stiffness only in compressive direction. The numerical results are consistent with the experiment. The problem of delamination instability is discussed through energy release rate.

Keywords : Composite plate, Postbuckling, Multiple delaminations, Energy release rate, Finite element analysis, Contact problem.

1. INTRODUCTION

It is one of the most important issues in the design of composite structures to solve Compression After Impact (CAI) problem, because the decreased compressive strength is often a critical concern. Since delaminations due to the impact are thought to be the main reason for a significant reduction in the compressive strength of composite laminates, the effect of the delamination(s) on the compressive behavior has been studied by many researchers. The finite element method has often been applied to the problems of buckling, postbuckling, and stability of delamination crack(s) due to its effectiveness in handling problems with complex conditions such as contact condition. One dimensional beam-type models of delaminated laminates have been studied by many researchers including Suemasu et al. [1], using finite element analysis to investigate postbuckling behavior and the stability of the delaminations as the problem is, at most, two dimensional in nature and thus does not require excessive numerical effort. These

studies have shown the validity of the numerical method to be applied this class of problem, including nonlinear analysis, the contact problem, and to obtain the fracture mechanical parameter of the energy release rate. However, limited research has been conducted toward the two dimensional plate problem as two dimensional modeling of a delaminated plate requires a large numerical effort, particularly when the delamination crack stability is discussed. Whitcomb and Shivakumar [2] and Shahwan and Waas [3] investigated the postbuckling behavior of a surface delamination considering the contact problem. Klug et al. [4] studied the postbuckling behavior of a plate with an elliptical delamination using the plate finite element and discussed the stability problem of the delamination by considering the energy release rate distribution.

Impact tests (e.g., references 5) showed that multiple delaminations, being relatively small compared to the size of the plate, was introduced at the impact point of CF/epoxy plates with the compressive strength of the damaged plate being reduced significantly. The main cause of reduced compressive strength due to impact is believed to be the existence of multiple delaminations. Thus, the effect of multiple delaminations on the compressive behavior of composite plates needs to be understood.

Suemasu et al. [6] studied the effect of multiple delaminations on the compressive behavior of rectangular plates through a buckling analysis using Rayleigh-Ritz method and finite element analysis together with experimental observations. The experiment showed that the instability of delamination cracks could be a trigger for the final failure of the delaminated plate in postbuckling process. The postbuckling behavior and delamination stability must also be studied in order to predict the CAI strength. The energy release rates distribution is obtained along the delaminations and consistent with the failure of the plate observed in the experiment.

The diameters of the delaminations increase from the impact surface to the other one in the real impact damage and the size difference of the delaminations may play an important roll in the compressive behavior. Suemasu et al has been numerically investigated the problem by using finite element analysis [7,8,9]. In the present paper more numerical and experimental results are presented.

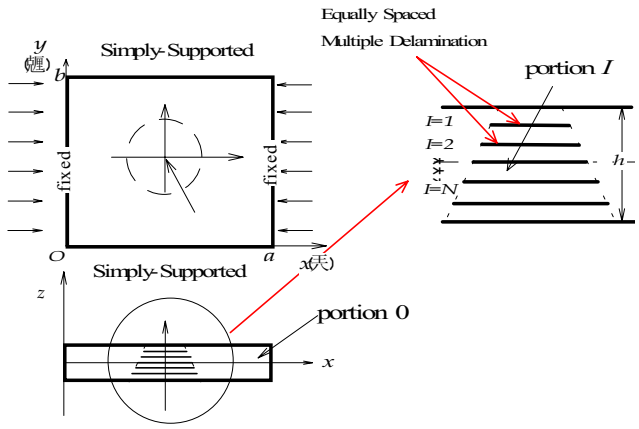

Fig.1 Analytical model of composite laminate with multiple delaminations of linearly varying diameter.

2. EXPERIMENT

An experiment was conducted to observe compressive behavior of the composite plates with different size circular delaminations. The test specimen is illustrated in Fig.2. The specimens were made of glass fiber plain-woven quasi-isotropic laminates in order to see the delamination propagation during the experiment. The stacking sequence was $[(0/45°//90°/-45°//)_2]_s$. The Young's modulus and Poisson ratio were measured to be about 17.2 GPa and 0.33. The

specimen thickness and the diameters of the delaminations are listed in Table 1. The specimens with dash such as D8A30' has a very large delamination near the back surface. The embedded delaminations were introduced by setting two Teflon sheets at the designated interfaces. Owing to the difficulty of placing the thin Teflon sheets at each interface during stacking each lamina, the plate thickness variation is not small from specimen to specimen. Teflon sheets were carefully placed on the designated plane to avoid sticking each other, but some polymer may soak into the gap of two sheets. Though the sticking force is thought to be very small, it affected the instability phenomena of the delaminated ligaments as mentioned later. Fig.3 is a schematic figure of the test set-up. The loading edges were clamped with two steel blocks and side edges were loosely supported by two blunt knife edges to realize fixed and simply-supported boundary conditions, respectively. The specimen was loaded by a very slow cross head speed of 0.1 mm/min before the deflection became large, then the speed changed to 0.5 mm /min. Applied load, center deflections of both surface, strains at several points and loading edge displacement were measured. Two non-contact laser displacement-meters were used to measure the center deflections.

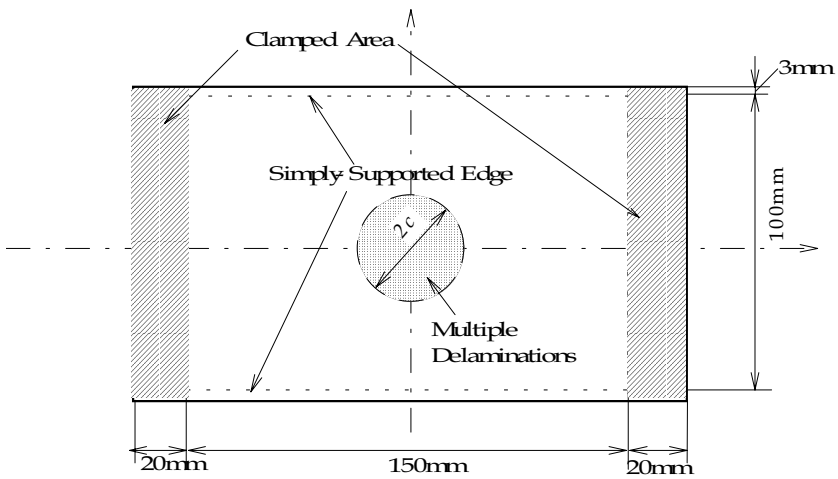

Fig.2 Test specimen of multiply delaminated plain-woven glass fiber laminates. The stacking sequence is $[(0/45/90/-45)_2]_s$.

Table 1 Diameters of the delamination and thickness of the specimens

Name	Diameters of delaminations (mm)	Thickness (mm)
D0-1	□	3.2
D0-2	□	3.7
D8S30	30×8	3.3
D8A20	12.5, 15, 17.5, 20, 22.5, 25, 27.5	3.3
D8A20'	12.5, 15, 17.5, 20, 22.5, 25, 37.5	3.4
D8A25	17.5, 20, 22.5, 25, 27.5, 30, 32,5	3.4
D8A25'	17.5, 20, 22.5, 25, 27.5, 30, 42,5	3.3
D8A30	22.5, 25, 27.5, 30, 32.5, 35, 37.5	3.6
D8A30'	22.5, 25, 27.5, 30, 32.5, 35, 47.5	3.1
D8A40	32.5, 35, 37.5, 40, 42.5, 45, 47,5	3.4
D8B40'	32.5, 35, 37.5, 40, 42.5, 45, 57,5	3.3
D8A45	37.5, 40, 42.5, 45, 47.5, 50, 52,5	3.4
D8B45'	37.5, 40, 42.5, 45, 47.5, 50, 62,5	3.3

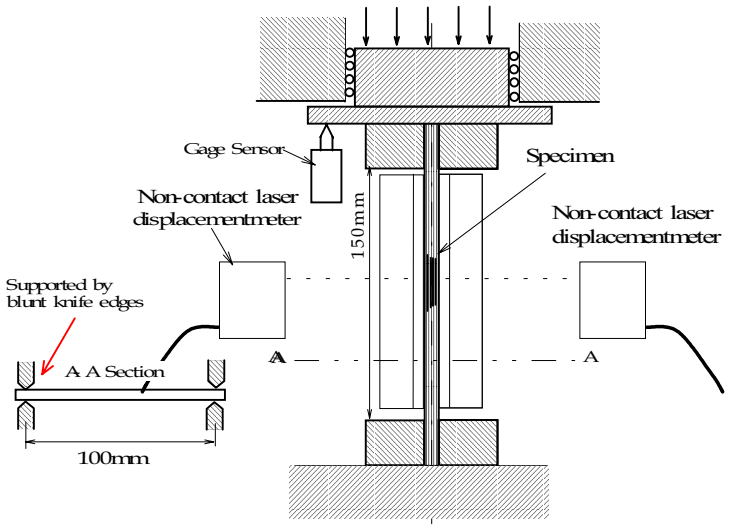

Fig.3 Experimental apparatus

The relationships between load and center deflection are plotted in Figs.4-8. Since the variation of the specimen thickness is not sufficiently small, the load and deflection are normalized by plate thickness h and a characteristic load P_0 $\{=Ebh(h/b)^2/(1-\nu^2)\}$. Fig.4 show the results of the intact plate. The specimen D0-1 buckled in a symmetrical shape and the center deflection increased with the compressive load until the plate showed an unstable snap-through buckling from symmetric to antisymmetric shape, while the specimen D0-2 changed the deformed shape gradually from symmetric to antisymmetric. It is why the specimen D0-2 had a large antisymmetric component in the initial imperfection.

The results for D8S30 and D8A30 are shown in Fig.5, both of which have almost equivalent damage. The sticking of the delamination disturbed the compressive behavior of both results. The buckling loads were well below the case of intact plate. D8S30 has very little delamination opening, while D8A30 show quite large opening of delamination. The initial buckling load of D8A30 looked much lower than that of D8S30, owing to the existence of larger surface delamination.

The relationships between the applied load and the center deflections of the front and back

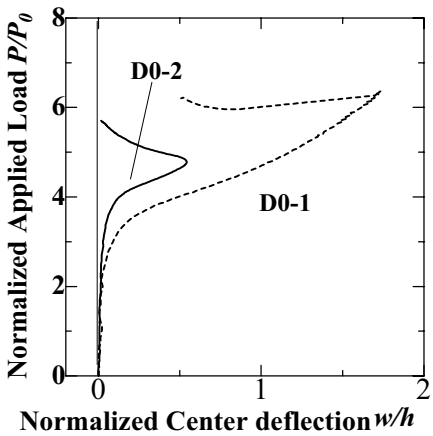

Fig.4 Relationships between normalized load and center deflection for intact specimens.

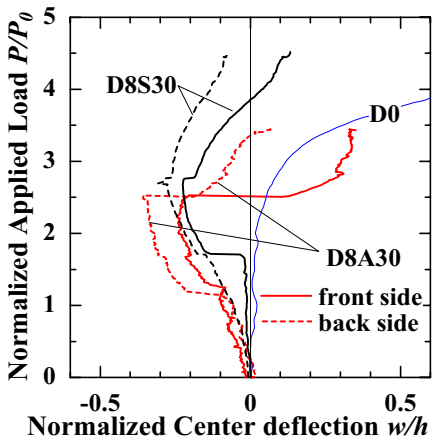

Fig.5 Relationships between normalized load and center deflection for D8S30 and D8A30

surfaces of the delaminated portions and those between the applied load and end shortening for delaminated specimens D8A20' and D8A20' are plotted in Figs. 6, 7. As mentioned earlier the specimen of D8A20' has a specially large delamination near the one surface. The compressive behavior basically consisted of four stages for both specimen, that is, 1.the pre-buckling state, 2.local buckling of only large delaminations, 3.symmetric global instability and 4. antisymmetric global instability. The unstable jump of the deflection at P/P_0~3.2 seen in specimen D8A20' is caused quite large unstable propagation of the delamination. Before the jumps of the deflection at higher load level there occurred some stable delamination propagation in the transverse direction. Specimens D8A20 and D8A20' show quite different compressive behaviors. The directions of the front side deflections were opposite probably due to global initial imperfection. D8A20' showed some unstable delamination propagation when P/P_0~3.2, while D8A20 had only stable delamination increase until final failure. The propagation became notable around a load level where the anti-symmetric deformation started to increase. The load level can be checked from the data of two strain gages glued at the points apart by same distance from the center of the plate. The stiffness reduction as a plate being almost negligible at the initial buckling became apparent with the increase of the load and significant when the antisymmetric deformation started to increase.

The results of D8A45 and D8A45' are shown in Fig.8. The deflection of back side of D8A45' started to increase at very low load owing to the existence of the large delamination compared to the cases D8A45, while the histories of the deflection of front side are similar to each other for both cases. The whole plate including intact portion tended to deform into the negative direction in a symmetric shape first. At this point quite large delamination

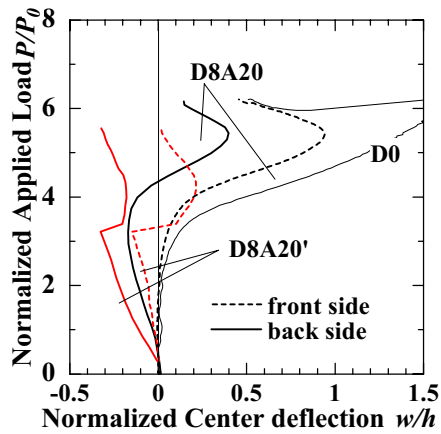

Fig.6 Relationships between normalized load and center deflection for D8A20 and D8A20'

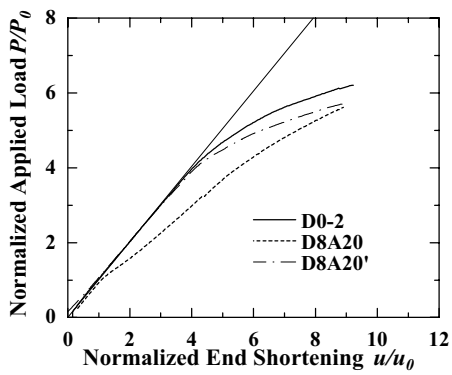

Fig.7 Relationships between normalized load and end shortening for D8A20 and D8A20'

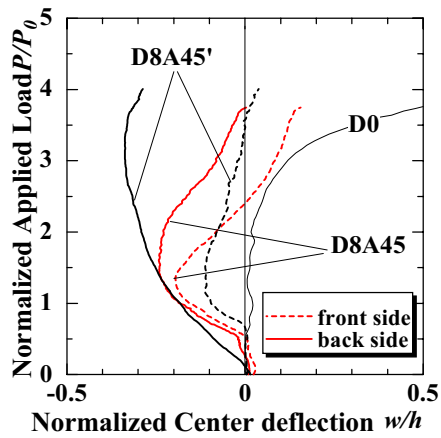

Fig.8 Relationships between normalized load and center deflection for D8A45 and D8A45'

opening appear particularly for D8A45'.

A picture of a damaged plate is shown in Fig.9. The delaminations I=6 and 7 propagated a little in the transverse direction.

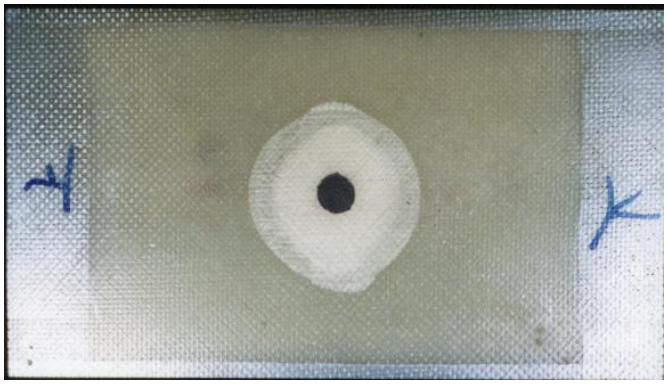

Fig.9 The damaged state of the specimen D8A30'.

3. FINITE ELEMENT ANALYSIS

The delaminated plates illustrated in Fig.1 were numerically analyzed using a finite element method (ABAQUS/ standard) in order to study the effect of size difference of the multiple delaminations on the buckling, post-buckling and failure mechanisms. The types of the plates analyzed are D8A30, D8A30', D8A45 and D8A45'. The failure mechanism was discussed fracture mechanically by using energy release rates obtained through the virtual crack closure technique. Considering that the plate suggested to be used for CAI test is quasi-isotropic and the effect of elastic properties in the thickness direction on compressive behavior is not usually significant [6], the material was assumed to be isotropic (E=41.9 GPa, ν=0.31) for simplicity. A three dimensional isoparametric 20-node brick element and 15-node wedge element (just at the center of the delaminated portions) was used as illustrated in Fig.10. As the deformation was symmetric about the center-line parallel to the loading direction, only a half of the plate was analyzed. The nodal displacement normal to the surface was constrained on the cross-section of the symmetry in order to satisfy the symmetric condition. On the simply-supported edge, the out-of-plane displacement of the nodes on the center line of the side boundary was constrained. At one of the fixed ends, the displacement in the loading direction was set to zero, while at the other end a uniform displacement in the loading direction was applied. Instead of considering an initial imperfection, small concentrated loads were applied at two points on the centerline of the intact portion and the center of each delaminated portion as shown in Fig.10. Owing to this initial transverse load, the plate deflected by the order of 1/20 of its thickness and all the delaminations had small opening. In order to consider the contact problem on the delaminated surface, a spring element was used between nodes on the upper and lower delaminated surfaces, which had a large reaction force when the relative displacement in the thickness direction Δw was negative and no force when the relative displacement was positive. The present spring element was an approximation of the contact problem and valid when the deflection was moderate.

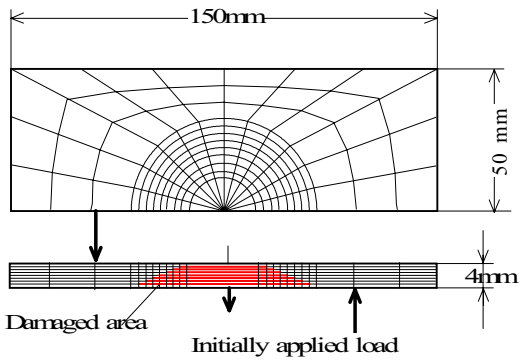

Fig.10 Finite element mesh

The present calculation was quite difficult and needed a large numerical effort, because not

only a geometrical nonlinearity but also the contact problem on all the delaminated surfaces must be considered in the three dimensional finite element analysis. Compressive behavior was calculated by increasing the uniform displacement of the loading edge with an increment which was automatically given to be small enough to ensure convergence. The convergence was normally most difficult to achieve at the region just prior to and following buckling. At this load level, contact areas were thought to change rapidly upon only small change in loading due to rapid shape change. Thus, the calculation should be initiated from a shape where all delaminations are open and no contact exists. Energy release rates are obtained using the virtual crack closure technique [10] for three-dimensional body.

3.RESULTS AND DISCUSSIONS

Center deflection of an intact plate is compared with the experiment in Fig.11. The experimental result was much lower than the analysis due to incomplete fixed condition at the loading edges and the low transverse shear rigidity of the specimen. The finite element analysis was stopped due to the difficulty of the convergence at $P/P_0 \approx 7$, which may be caused by the existence of the unstable path as observed in the experiment.

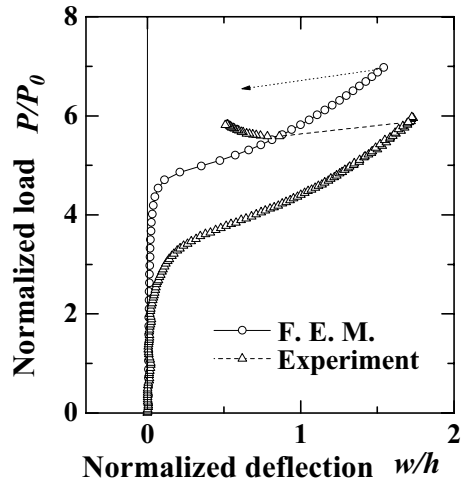

Fig.11 Comparison of the results obtained by present formulation and usual finite element formulation

The normalized buckling loads are compared in Table 3. The buckling load reduction obtained from the finite element analysis qualitatively coincided with those of the experiment.

Table 3 Normalized buckling load by P_0 ($P_0=Ebh(h/b)^2/\{(1-\nu^2)\}$)

Specimen	Normalized Buckling load	
	Experiment	F. E. A.
D0	3.45	4.92
D8A30	>1.31	0.89
D8A30’	1.0	0.55
D8B	0.53	0.47
D8B'	0.48	0.40

Center deflections of delaminated plates mentioned in the former section are plotted against the applied load in Fig. 12. Only the case D8A30’ finally moved to positive direction with quite large delamination opening, while the other cases moved to the negative direction with small delamination opening. Both type of the deformation histories were observed in the experiment probably due to the difference of initial imperfection. The global deformation still tended to change from symmetric one-wave shape to two-wave shape after some increase of symmetric deformation. However, the deformation could not take perfect antisymmetric shape due to the lack of symmetry of the present model. This is different from the behavior of the plate with equal size multiple delaminations. When there existed a particular large delamination, the deflection started increasing at very low load owing to the buckling of the large delaminated portion. The large delamination tended to open in postbuckling. Typical deformation histories of D8A30 and D8A30' are shown in Figs.13 and 14.

The relationships between the load and the loading edge displacement are plotted in Fig.15. The inplane stiffness decreased too little just after the initial buckling of the delaminated portions to find the buckling from the figure. The stiffness reduction became apparent when the smallest delaminated portion started to deflect (P≈70kN for D8A30 and D8A30', P≈25kN for D8A45 and D8A45'). The stiffness reduction finally became significant when the deformation of the intact portion became notable. This means that buckling of the largest delaminated ligament may not contribute to the significant reduction of the CAI strength and the instability of the small other delaminated ligaments may be more important factor of the CAI problem. We may say that we should use the average damage size through the thickness of the plate instead of projected damage area size as the measure of the significance of the impact damage, because the projected area only means the size of the largest delamination.

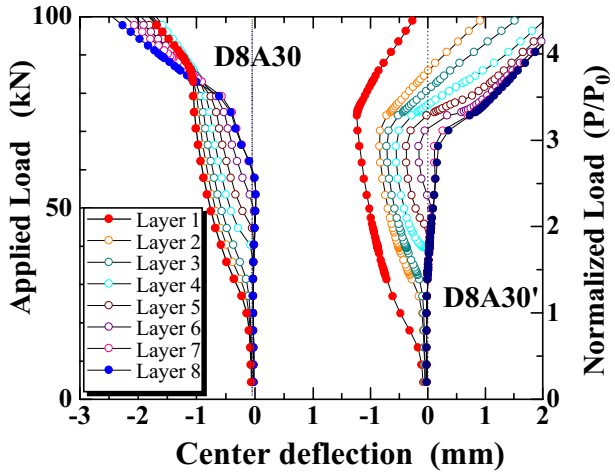

(a)

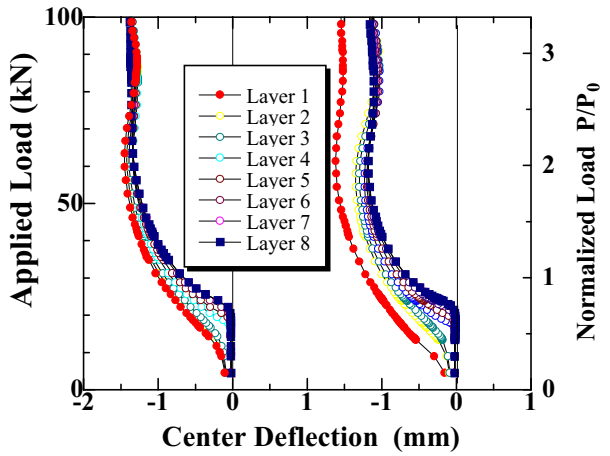

(b)

Fig.12 Relationship between the load and center deflections for the plates with seven delaminations
(a)D8A30, D8A30', (b) D8A45, D8 A45'

The energy release rate distribution along the delamination edges for the model D8A30' is plotted in Fig.16. Just after the buckling (P=27 kN) the energy release rate increased only at the delamination No. 1 and was negligible at the other delaminations, because only the largest delaminated portion deformed. The mode *I* component was dominant owing to the large delamination opening. At the load of *P*=50 kN

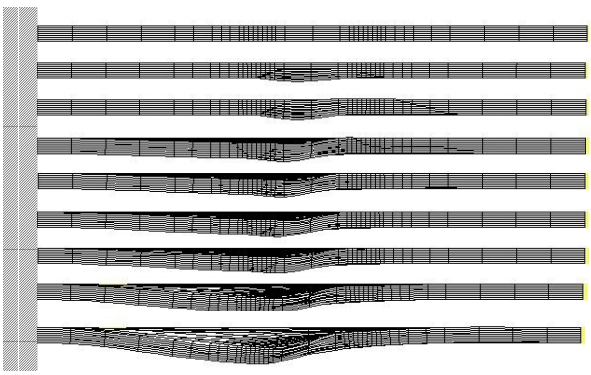

Fig.13 Deformed shape change with the increase of the load for D8A30

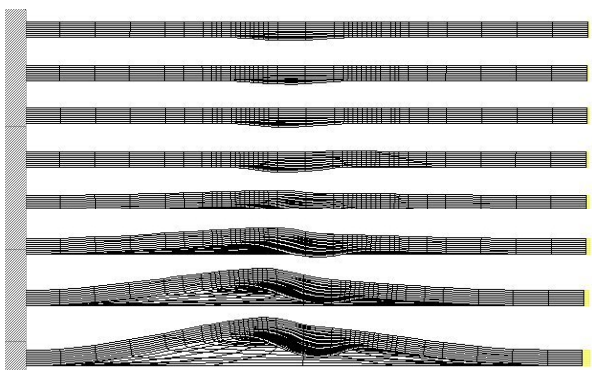

Fig.14 Deformed shape change with the increase of the load for D8A30'

where the smallest delaminated portion just started to deform, the energy release rate still maximum at the largest delamination. The value was sufficient for the delamination of the conventional CFRP laminates to propagate. The load level was less than 1/3 of the buckling load of the intact laminates. In the case of D8A30, being not shown here owing to the space limitation, the mode III component was dominant at this load level.

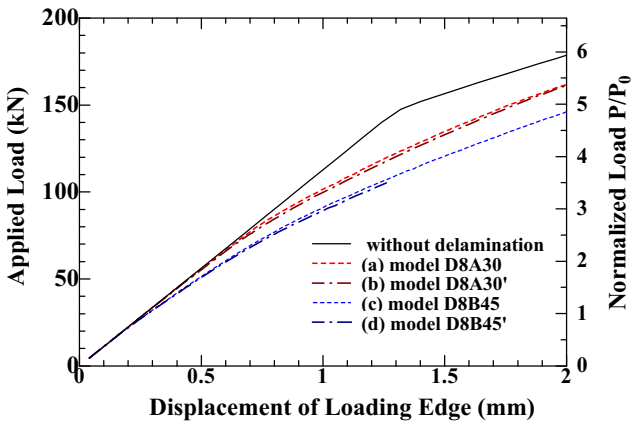

Fig.15 Relationships between the load and end-shortening

Total energy release rate at the transverse edge of the largest delamination is plotted against the applied load in Fig.17. The energy release rate increased rapidly with the load after the instability of the small delaminated portions. The energy release rate level reached at the level of interlaminar toughness of the conventional CFRP laminates before the intact portion became unstable and laminate was still symmetric deformation. The results well explained that the delamination propagation observed at the largest delamination front at the transverse edges of the laminate in the experiment.

CONCLUSIONS

A model experiment and finite element analysis were performed to investigate the failure mechanism of the multiply delaminated plate. The finite element analysis well explained the experimental results, that is, the buckling load reduction, the failure due to the instability of delaminations, etc. The following conclusions are noted.

1. Plates with multiple delaminations buckled with a symmetric shape. However, their shape changed significantly during loading.
2. The compressive strength of the composite plate with multiple delaminations, whose failure was initiated by delamination propagation in the transverse direction, may be well predicted by the energy release rate distribution.
3. The energy release rate increases rapidly when the small delaminated ligament start to deform.

Acknowledgments

The present research is supported by Ministry of Education, Science and Culture, Japan (Grant Aid for Scientific Research(C) No. 09250765).

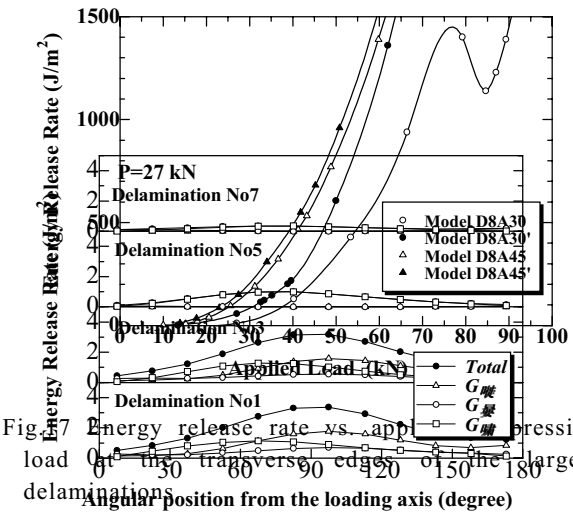

Fig.17 Energy release rate vs. applied compressive load at the transverse edges of the largest delaminations

References

1. Suemasu H., Finite element analysis of compressive behaviors and delamination crack

instability of multiply delaminated cross-ply laminates, Journal of Japan Society for Aeronautical and Space Sciences, Vol.43, No.500, September 1995, 513-519.

2. Whitcomb, J. D. and Shivakumar, K.N., Strain-energy release rate analysis of plates with postbuckled delaminations, Journal of Composite Materials, Vol.23, July 1989, 714-734.
3. Shahwan K.W. and Waas A.A., A mechanical model for the buckling of unilaterally constrained rectangular plates, International Journal of Solids and Structures, Vol.31, No.1, 1994, pp.23-37.
4. Klug J., Wu X.X and Sun C.T., Efficient modeling of postbuckling delamination growth in composite laminates using plate elements, AIAA J. Vol.34, No.11, January 1996, 178-184.
5. Ishikawa T., Sugimoto S. Matsushima M. and Hayashi Y., Some experimental findings in compression after impact (CAI) tests of CF/PEEK(APC-2) and conventional CF/epoxy flat plates, Composite Science and Technology, 55, 1995, 349-363.
6. Suemasu H., Kumagai T. and Gozu K., Compressive behavior of rectangular composite laminates with multiple circular delaminations, I. Experimental and analytical development, II. Finite element analysis, AIAA Journal, Vol.36, No.7, 1279-1290, 1998.
7. Suemasu H., Morita K. and Majima O., Compressive behavior of rectangular composite laminates with multiple delaminations of different sizes, Proceedings of AIAA/ASME/ASCE/AHS/ASC, 39th Structures, Structural Dynamics, and Materials Conference, 1998.
8. H. Suemasu, H. Wakabayashi, K. Nakamura and O. Majima, Effect of different size multiple delaminations on compressive behavior of composite laminates, Proceedings of AIAA/ASME/ASCE/AHS/ASC, 40th Structures, Structural Dynamics, and Materials Conference, 1999.
9. H. Suemasu, H. Wakabayashi, K. Nakamura and O. Majima, Failure Mechanism of Composite Laminates with Different size multiple delaminations Subjected to Compressive Load, Proceedings of AIAA/ASME/ASCE/AHS/ASC, 41st Structures, Structural Dynamics, and Materials Conference, 2000.
10. Shivakumar, K. N., Tan P. W. and Newman J. C., A virtual crack-closure technique for calculating stress intensity factors for cracked three dimensional bodies, International Journal of Fracture, 36, 1988, R43-R50.